Investigation of the Functional Effects of KCNJ2-linked Short QT Syndrome on Electrical Conduction at Purkinje-ventricle Junction at Low- and High- Frequencies

Cunjin Luo[1], Kuanquan Wang[1], Qingjie Wang[2], Yongfeng Yuan[1], Qince Li[1], Zhili Li[3], Ming Yuan[3], Henggui Zhang[1,4]

[1]School of Computer Science and Technology, Harbin Institute of Technology, Harbin, China
[2]Department of Cardiology, Zhongda Hospital of Southeast University, Nanjing, China
[3]State Key Lab of Space Medicine Fundamentals and Application, China Astronaut Research and Training Center, Beijing, China
[4]School of Physics and Astronomy, the University of Manchester, Manchester, UK

Abstract

Recent studies suggested that genetic KCNJ2-linked short QT syndrome (SQT3) arises due to I_{K1} mutations leading to accelerated ventricular repolarization, arrhythmias. However, ionic mechanisms underlying cardiac arrhythmias of SQT3 are incompletely understood. Our goal was to investigate the functional impacts of SQT3 on the electrical wave conduction at the Purkinje-ventricle junction (PVJ). In the computational simulations, compared with 1.25 Hz of electrical stimulation, the measured APD_{90} did not change noticeably at 0.5 Hz, but was reduced at 2.66 Hz. At 3.33 Hz, 1:1 response of electrical excitation wave propagation to stimuli failed in WT condition, but sustained in mutation conditions. This suggested that increased I_{K1} accelerates ventricular repolarization, and reduces APD spatial dispersion along the tissue, which facilitates the conduction of rapid electrical excitation waves in contrast to conduction failure in the WT condition. Such a loss of protective effect at high frequency of electrical stimulation, together with abbreviated APD and ERP, may account for the initiation of ventricular tachycardia and fibrillation.

1. Introduction

The short QT Syndrome (SQTS) is an inherited cardiac channelopathy associated with increased risks of malignant ventricular arrhythmias. SQT3 is identified as a genetic mutation, in which aspartic acid is replaced by asparagines at position 172 in the Kir2.1 potassium channel [1]. In their study, El Harchi et al. [2] have shown the Kir2.1 D172N mutation resulted in preferential augmentation of the outward current based on data from whole-cell patch-clamp recordings of Kir2.1 current at ambient and physiological temperatures. Further studies [3] have shown that SQT3 mutation abbreviated action potential duration (APD) and effective refractory period (ERP), and steepened the APD and ERP restitution curves, which consequently shortened the QT interval and modified the T wave characteristics on the pseudo-ECG.

Ionic mechanisms underlying mechanisms of SQT3 has not been understood thoroughly despite lots of effect have been done. In this study, we investigated the functional impacts of SQT3 on the electrical wave conduction at the Purkinje-ventricle junction (PVJ) at low-(0.5Hz), normal-(1.25Hz), and high-(2.66Hz, 3.33Hz) frequency of electrical stimulation. Using this PVJ model, rate-dependent effects of the KCNJ2 mutations on cardiac electrophysiology and AP wave conduction were examined. The obtained results provided new insights towards understanding the mechanisms by which the Kir2.1 D172N mutation abbreviated APD and ERP, which may account for the initiation of ventricular tachycardia and fibrillation.

2. Materials and methods

2.1. Governing equation of electrical wave propagation in 2D cardiac Purkinje-venticle tissue

In this section, a multi-cellular model of 2D human Purkinje-ventricle tissue was constructed by incorporating Stewart et al. [4] Purkinje fibre model and the ten Tusscher et al. [5] ventricular model into a reaction diffusion partial differential equation (Eq. 1). To represent the heterogeneous electrophysiological properties, we used a standard mono-domain description for cardiac tissue:

$$\frac{\partial V_m}{\partial t} = -\frac{I_{ion} + I_{stim}}{C_m} + \nabla \cdot (D\nabla V) \quad (1)$$

where V_m is transmembrane potential, C_m is the membrane capacitance, I_{stim} is the externally applied stimulus current, and D is the diffusion tensor, is the gradient operator, t is time, I_{ion} is the sum of ionic currents as described in the following equation:

$$I_{ion} = I_{Kr} + I_{Ks} + I_{K1} + I_{to} + I_{Na} + I_{bNa} + I_{CaL} + I_{bCa} + I_{NaK} + I_{NaCa} + I_{pCa} + I_{pK} + I_{NaL} \quad (2)$$

The modified ventricular cell model was incorporated into the cardiac tissue model of Eq.1. In the present study, equations of I_{K1} were modified for three main situations: wide type (WT), heterozygous (WT-D172N) and homozygous (D172N), which are described as follows [3]:

$$I_{k1} = G_{k1}\sqrt{\frac{K_o}{5.4}}x_{k1\infty}(V - E_k) \quad (3)$$

$$x_{k1\infty} = \frac{\alpha_{k1}}{\alpha_{k1} + \beta_{k1}} \quad (4)$$

WT:

$$\alpha_{k1} = \frac{0.07}{1 + e^{0.017(V - E_k - 200.2)}} \quad (5)$$

$$\beta_{k1} = \frac{3e^{0.0003(V - E_k + 100.2)} + e^{0.08}(V - E_k - 8.7)}{1 + e^{-0.024(V - E_k)}} \quad (6)$$

$$G_{k1} = 4.8ns / pF \quad (7)$$

WT-D172N:

$$\alpha_{k1} = \frac{0.1}{1 + e^{0.023(V - E_k - 199.9)}} \quad (8)$$

$$\beta_{k1} = \frac{3e^{0.0002(V - E_k + 100.4)} + e^{0.07(V - E_k - 9.8)}}{1 + e^{-0.02(V - E_k)}} \quad (9)$$

$$G_{k1} = 6.27ns / pF \quad (10)$$

D172N:

$$\alpha_{k1} = \frac{0.1}{1 + e^{0.05(V - E_k - 199.9)}} \quad (11)$$

$$\beta_{k1} = \frac{3e^{0.0002(V - E_k + 100.1)} + e^{0.08(V - E_k - 10.3)}}{1 + e^{-0.006(V - E_k)}} \quad (12)$$

$$G_{k1} = 11.32ns / pF \quad (13)$$

where G_{k1} is the maximal channel conductance of I_{k1}, $x_{k1\infty}$ is the time-independent inward rectification factor, K_o is the extracellular potassium concentration.

In this study, we included connections between Purkinje fibers and ventricular cells via gap junctions, which allowed studying ventricular excitation driven by the Purkinje fibres. The model was comprised of a Purkinje fiber region (cells 40 × (1~50)), an endocardial region (cells 40 × (51~71), an M-cells region (cells 40 × (76~110)), and an epicardial region (cells 40 × (111~150)). It represented a transmural width of ventricle (0.4 cm × 1.5 cm), consisting of 25% Endo cells, 35% M cells and 40% Epi cells. The proportion of different cells in this study is the same as that used in previous studies [3,6,7,8]. All the 2D simulations were carried out in an isotropic domain with D=0.1, a time step of 0.02 ms and space steps of 0.2 mm in both x and y directions. These 2D partial differential equations were solved by the forward Euler method.

2.2. Computing the pseudo-ECG

The pseudo-ECG was calculated as an integral of gradient of membrane potential at all positions on the virtual tissue from a virtual electrode located in the extracellular space following the methods used by other studies [3, 6], which was computed as following:

$$\Phi = \int \frac{D\nabla V_m \cdot \vec{r}}{r^3} dV \quad (14)$$

where Φ is electrical potential, V is the area of 2D tissue. $\vec{r}$ is the vector from the recording electrode to a point in the tissue. In this paper, we placed the virtual electrode at the left side of the central region of the tissue, 2 cm distance off the endocardial layer cells.

3. Results

3.1. Tables

In this study, we simulated electrical wave conduction, stimulated at low-, normal-, and high-frequencies in WT, WT-D172N and D172N conditions using a 2D human Purkinje-ventricle tissue model. Fig. 1 Shows the APD_{90} across the strand in the middle of the 2D sheet tissue stimulated at low-, normal-, and high-frequencies in WT, WT-D172N and D172N conditions. Compared with 1.25 Hz frequency (BCL=800ms) of electrical stimulation, the measured APD_{90} across the strand did not change noticeably at 0.5 Hz (BCL=2000ms), but was reduced at 2.66 Hz (BCL=375). Compared with the WT condition, the APD_{90} across the strand was reduced in the WT-D172N and D172N conditions (Fig. 1). Fig 2 shows the APD_{90} dispersion across the strand. The increased I_{K1} due to the D172N mutation accelerated ventricular repolarization, and reduced APD spatial dispersion at PVJ. Then we calculated the conduction velocity in the Purkinje fibre, Purkinje-ventricular junction, and ventricular tissue in WT, WT-D172N, and D172N conditions as shown in Fig. 3. Fig. 4 shows simulated pseudo-ECG at high- and normal-frequencies in WT, WT-D172N and D172N conditions. At 3.33 Hz of pacing rate, electrical excitation wave propagation failed 1:1 in response to stimuli in WT condition, but sustained in

WT-D172N and D172N conditions. Our simulation results indicated that in Kir2.1 D172N mutation condition, ventricular tachycardia is more easily initiated at high frequency. These results demonstrated that the Kir2.1 D172N mutation affects ventricular tissue's excitability, which may be pro-arrhythmic.

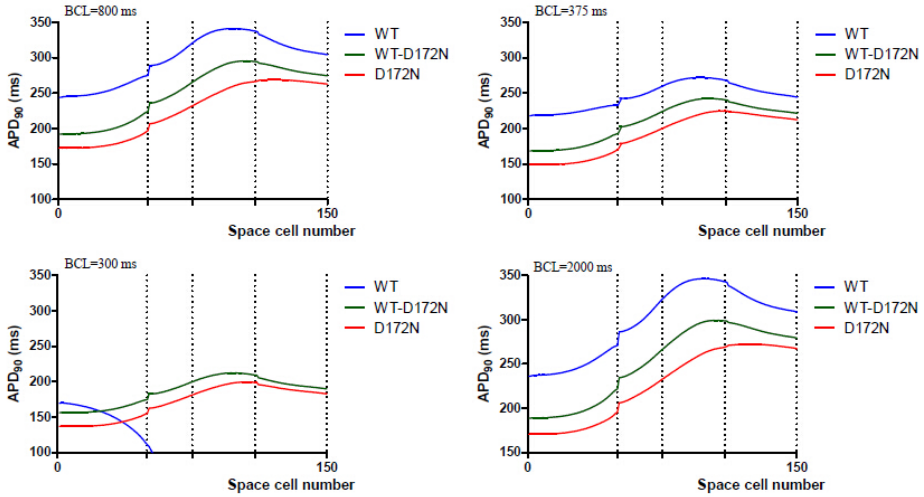

Fig. 1. APD_{90} across the Purkinje-ventricle tissue at low-, normal-, high- frequencies

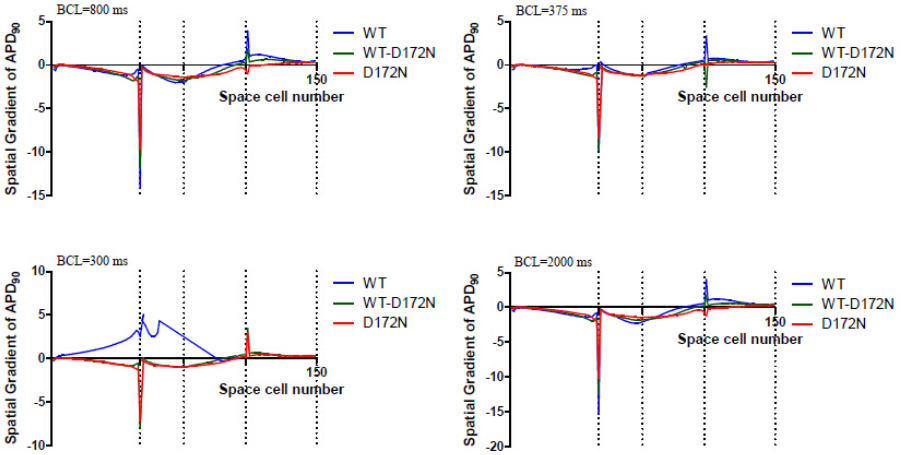

Fig. 2. Spatial gradient of APD_{90} across PVJ at low-, normal-, high-frequencies

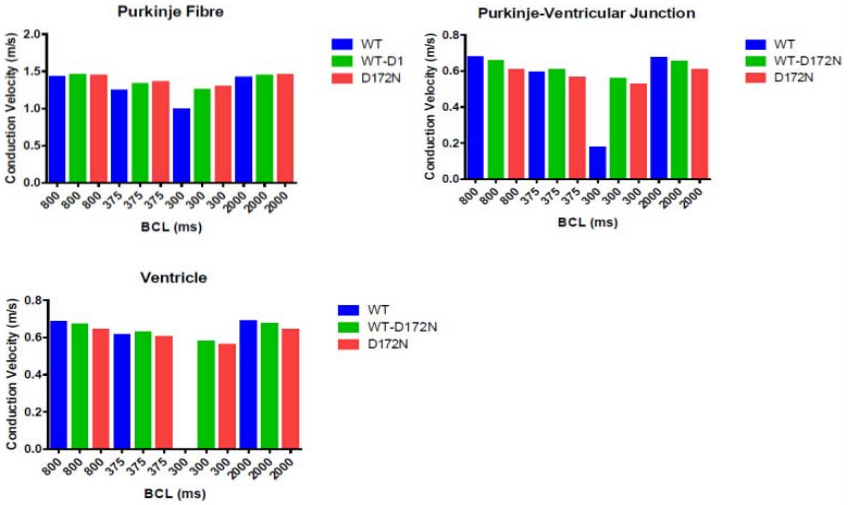

Fig. 3. Conduction velocity in different areas in WT, WT-D172N and D172N conditions.

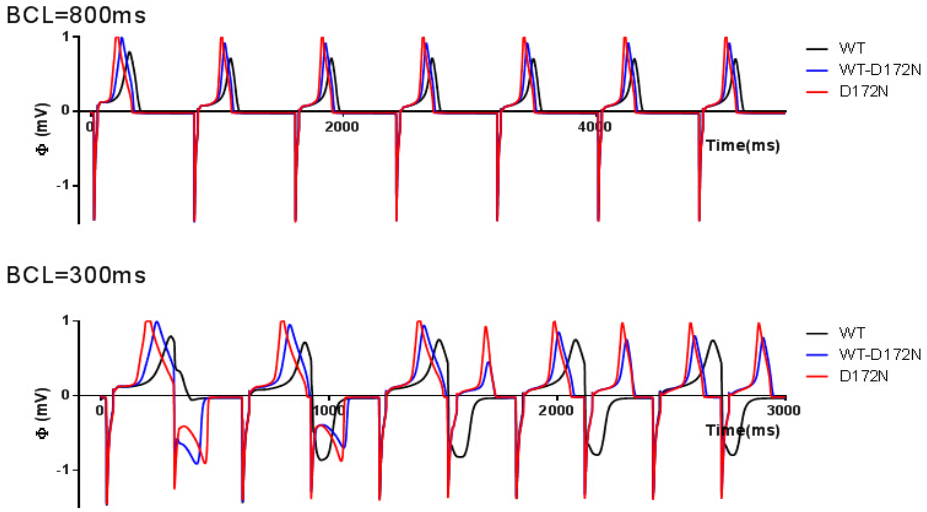

Fig. 4. Simulated pseudo-ECG at high- and normal-frequencies.

4. Discussion

In this study, we delineated the effect of SQT3 on electrical wave conduction at Purkinje-ventricle junction at low- and high- frequency by using a computational model that based on an electrophysiological model of 2D tissue. Since the only difference between these simulation conditions was the change of I_{K1} channel kinetics, the increased I_{K1} due to the D172N mutation accelerated ventricular repolarization, and reduced APD spatial dispersion along the Purkinje-ventricle tissue, which otherwise fails to conduct in the WT condition. Such a loss of protective effect of cardiac tissue to high frequency of electrical stimulation, together with abbreviated APD and ERP, may account for the initiation of ventricular tachycardia and fibrillation.

Acknowledgements

This study was supported in part by the National Natural Science Foundation of China (NSFC) under Grant No. 61179009, No. 61173086, and also supported by China Scholarship Council (CSC).

References

[1] Priori, SG, Pandit SV, Rivolta I, Berenfeld O, Ronchetti E, Dhamoon A, Napolitano C, Anumonwo J, Di Barletta MR, Gudapakkam S, Bosi G, Stramba-Badiale M &Jalife J.A novel form of short QT syndrome (SQT3) is caused by a mutation in the KCNJ2 gene. Circ Res 2005; 96: 800-7.

[2] EL Harchi A, Mcpate MJ, Zhang Y, Zhang H &Hancox JC. Action potential clamp and chloroquine sensitivity of mutant Kir2.1 channels responsible for variant 3 short QT syndrome. J Mol Cell Cardiol 2009; 47: 743-7.

[3] Adeniran I, EL Harchi A, Hancox JC & Zhang H. Proarrhythmia in KCNJ2-linked short QT syndrome: insights from modelling. Cardiovasc Res 2012; 94: 66-76.

[4] Stewart P, Aslanidi OV, Noble D, Noble PJ, Boyett MR, et al. Mathematical models of the electrical action potential of Purkinje fibre cells. Philos Trans A Math Phys Eng Sci 2009, 367: 2225-2255.

[5] Ten Tusscher KH &Panfilov AV. Alternans and spiral breakup in a human ventricular tissue model. Am J Physiol Heart CircPhysiol 2006; 291: H1088-100.

[6] Wang K, Luo C, Wang W, Zhang H, Yuan Y. Simulation of KCNJ2-linked short QT syndrome in human ventricular tissue. Computing in cardiology 2013; 40: 349-352.

[7] Wang K, Luo C, Yuan Y, Lu W, Zhang H. Simulation of re-entrant wave dynamics in a 2-D sheet of human ventricle with KCNJ2-linked variant 3 short QT syndrome. Computing in cardiology 2014; 41: 61-64.

[8] Zhang H &Hancox JC. In silico study of action potential and QT interval shortening due to loss of inactivation of the cardiac rapid delayed rectifier potassium current. Biochem Biophys Res Commun 2004; 322: 693-9.

Address for correspondence.
Kuanquan Wang (wangkq@hit.edu.cn)
Mailbox: 332,
Harbin Institute of Technology,
Harbin 150001,
China.